BESSM, 2023, Vol 7, No 1, 26-31
https://doi.org/10.54987/bessm.v7i1.899

HIBISCUS PUBLISHER

BULLETIN OF ENVIRONMENTAL SCIENCE & SUSTAINABLE MANAGEMENT

Website: http://journal.hibiscuspublisher.com/index.php/BESSM/index

BESSM VOL 7 NO 1 2023 Azokeratin

Modelling the Inhibitory Effect of Mercury on the Growth Rate of a Bacterium on Acrylamide

Motharasan Manogaran[1,2]*, Syahir Habib[1,3], Mohd Badrin Hanizam Abdul Rahim[1,3], Aisami Abubakar[4], Umar Abubakar Muhammad[5] and Ibrahim A. Allamin[6]

[1]Department of Biochemistry, Faculty of Biotechnology and Biomolecular Sciences, Universiti Putra Malaysia, 43000 Kajang, Selangor, Malaysia.
[2]Malaysia Genome and Vaccine Institute (MGVI) National Institute of Biotechnology Malaysia (NIBM) Jalan Bangi, 43000 Kajang, Selangor, Malaysia.
[3]Agribiotechnology Group, Faculty of Biotechnology and Biomolecular Sciences, Universiti Putra Malaysia, UPM 43400 Serdang, Selangor, Malaysia.
[4]Department of Biochemistry, Faculty of Science, Gombe State University, P.M.B 127, Tudun Wada, Gombe, Gombe State, Nigeria.
[5]Department of Biological Sciences, Faculty of Science, Gombe State University, P.M.B 127, Tudun Wada, Gombe, Gombe State, Nigeria.
[6]Department of Microbiology, Faculty of Science, University of Maiduguri P.M.B 1069 Maiduguri, Nigeria.

*Corresponding author:
Dr. Motharasan Manogaran,
Malaysia Genome and Vaccine Institute (MGVI),
National Institute of Biotechnology Malaysia (NIBM),
Jalan Bangi,
43000 Kajang,
Selangor,
Malaysia.
Email: motharasan@gmail.com

HISTORY

Received: 24th May 2023
Received in revised form: 5th July 2023
Accepted: 30th July 2023

KEYWORDS

Mercury
Acrylamide-degrading bacterium
Pseudomonas
Inhibition kinetics
Mathematical models

ABSTRACT

Mercury was a potent inhibitor of the acrylamide-degrading *Pseudomonas* sp. strain DrY Kertih bacterium. The bacterium is capable of growing on acrylamide as a nitrogen source. Growth shows a sigmoidal pattern with lag times of 7–10 hours when exposed to increasing amounts of mercury. Bacterial growth was significantly slowed down while the lag period was increased as the concentration of mercury was increased to 0.1 mg/L, and eventually, growth stopped altogether. Growth rates at various mercury concentrations were calculated using a modified Gompertz model to obtain the maximum specific growth rate parameter. The modified Han-Levenspiel, modified Andrews, Shukor, Kai, Liu, Wang and Amor models were applied to the growth rates. The Amor model was unable to fit the curve. The Wang model performed the best statistically, with the lowest RMSE and AICc, the highest adjusted correlation coefficient (adR^2), and AF and BF values closest to unity. The parameters obtained were K_c, μ_{max} and m which represent critical heavy metal ion concentration (g/l), and maximum growth rate (g/l h) and empirical constant values were K_C, μ_{max} and m which represent inhibition constant (mg/L), maximum growth rate (per h) and empirical constant values were 0.054, 0.431 and 4.295, respectively. The results obtained in this study are useful when remediation works on polluted sites containing acrylamide co-contaminated with metal ions especially mercury.

INTRODUCTION

Acrylamide-induced seminiferous tubule histological abnormalities damage male rats' reproductive systems. Chemicals produce histological abnormalities. If inhaled or ingested, acrylamide may produce burning or a rash. Overactive sweating, sluggishness, and tongue trembling indicate neurological issues [1]. Acrylamide binds to DNA and mouse protamine during the spermatogenic process in mice, causing genetic diseases [2]. Research has connected acrylamide exposure in rats to endocrine-related malignancies, perinatal mortality, clastogenicity, mutagenicity, and male reproductive toxicity [3]. Spencer and Schaumburg found that acrylamide exposure in experimental animals caused cancer, but it is unclear if the same is true for humans [1]. Yang et al. found that acrylamide may mutate Salmonella strains TA100 and TA98. Mice injected intraperitoneally with 50 mg/kg acrylamide showed more chromosomal abnormalities in their bone marrow [4]. Acrylamide intraperitoneal doses up to 125 mg/kg did not increase chromosomal abnormalities in mice lymphocytes.

Intraperitoneal acrylamide was found to cause this [5]. Acrylamide can be absorbed through the lungs, skin, placental barrier and the digestive system due to its high water solubility. Acrylamide adducts in haemoglobin can be used to estimate the public's exposure to acrylamide due to their profession. According to the data, 41 acrylamide industrial workers had haemoglobin adduct-related neurotoxicity. Haemoglobin adducts surged in workers from a Chinese acrylamide plant, indicating that they were exposed to exceptionally high amounts of acrylamide [6]. Japanese water contamination cases have caused many cases of acute acrylamide poisoning. Multiple individuals have experienced this [7]. Five persons with truncal ataxia and disorientation symptoms were found to consume the acrylamide-poisoned water.

Acrylamide, a neurotoxic and carcinogenic chemical, can develop during the Maillard reaction. Carbohydrate-heavy foods cooked at high temperatures can produce acrylamide. Acrylamide is produced by the Maillard process in carbohydrate-rich meals. The Maillard process begins when carbohydrates in food and amino acids are mixed at a very high temperature especially frying [8]. Acrylamide-contaminated streams in Sweden and Norway killed cattle and fish. Polyacrylamide (PAM) is the most prevalent use for acrylamide in the production of adhesives, plastics, printed goods, and drinking water. As of 2005, commercial polyacrylamides often contain the deadly monomer of acrylamide, which has had a major impact on our food supply chain. Roundup pesticide pollutes agricultural soil with 30% polyacrylamide. This issue must be remedied by biologically remediating acrylamide as one of the most efficient methods [9].

Toxic metal ions in polluted wastewater inhibited bacterial growth and acrylamide use. Heavy metals hinder biodegradation and bioremediation. Heavy metal ions, unlike many other inhibitors, cannot be degraded, therefore when microbes accumulate a dangerous amount, their growth rate is inhibited. Thus, hazardous ion inhibitory characteristics can be examined using substrate inhibition model changes. Numerous models such as the modified Han-Levenspiel [10], Shukor [11], Wang [12], modified Andrews [13], Liu [14], Kai [15,16]Amor [17] have been utilised [18] to evaluate the result of heavy metal on the bacterial degradation of toxic substances [19–21]. The inhibition parameters obtained from this modelling will be very useful to understand the limitations of the biodegradation process.

Other than these observations, most studies on heavy metals and microorganism development focus on primary models. Mercury, silver, and copper substantially inhibited an isolated acrylamide-degrading bacteria [22,23]. This project uses multiple models of inhibition to investigate how mercury affects the development of this bacterium in the presence of acrylamide.

MATERIALS AND METHODS

Growth and maintenance of acrylamide-degrading bacterium

The acrylamide-degrading bacterium—*Pseudomonas* sp. strain DrY Kertih has been previously isolated in our lab [24]. Characterization of bacterial growth on acrylamide was performed using microtiter plates (Corning® microplate) [25,26]. The bacterium was grown on glucose as a sole source of carbon and in a basal salts (BS) medium containing the following: KH_2PO_4, (1.36 g l^{-1}), Na_2HPO_4, (1.39 g l^{-1}), $CaCl_2$ (0.01 g l^{-1}), $MgSO_4$ (0.01 g l^{-1}), and glucose (10 g l^{-1}) [27]. The final volume was 0.2 mL. Acrylamide was filter-sterilized (0.2 µm filter membrane Teflon) to a final concentration of 1.0 g L^{-1}. The microplates were incubated sealed at 30 °C resulting in static growth and the increase in turbidity due to bacterial growth was read at 600 nm (BioRad reader, model 680, Richmond, CA). The control contained everything minus acrylamide. The effect of mercury on the growth curve of the bacterium on acrylamide as the nitrogen source was carried out by adding mercury (Merck Atomic Absorption standard) from 0.01 to 0.1 mg/L final concentration.

Modified Gompertz model as the primary model in modelling growth on acrylamide

The modified Gompertz model is a predominantly fast convergence model that is commonly used to fit bacteria growth on toxic xenobiotics [28–32]. The prerequisite of using this model and other primary models to obtain the maximum specific growth rate is the values of growth, either in dry weight, A600nm, OD 600nm or CFU/mL have to be ln transformed [33–35], as the growth rate unit is per hour or per d. The equation is as follows;

$$y = A\exp\left\{-\exp\left[\frac{\mu_m e}{A}(\lambda - t)+1\right]\right\} \quad (1)$$

Inhibitory models for growth rate on acrylamide

The result of this preliminary modelling effort was utilized to model (**Table 1**) the influence of metal in the following models;

Table 1. Various growth inhibitory models.

Models	Equation	Authors
Modified Han-Levenspiel	$r = u_{max}\left(1 - \frac{C}{C_{crit}}\right)^m$	[10]
Wang	$r = \frac{u_{max}}{1 + \left(\frac{C}{K_C}\right)^m}$	[12]
Liu	$r = \frac{u_{max}K_C}{K_C + C}$	[14]
Modified Andrews	$r = \frac{u_{max}C}{K_s + C + \left(\frac{C^2}{K_i}\right)}$	[13]
Amor	$r = \frac{u_{max}C}{C + \left(\frac{C^2}{K_i}\right)}$	[17]
Shukor	$r = \upsilon_{max}\left(1 - \left(\frac{C}{S_m}\right)^n\right)$	[11]
Kai	$r = \upsilon_{max}\exp(-kx)$	[15]

Growth Fitting

CurveExpert Professional software was used in the modelling exercise. The software applies a Marquardt algorithm to the nonlinear equations (Version 1.6). To find the optimal solution, the algorithm looks for the smallest possible squared difference between the anticipated and actual numbers. The steepest ascent approach is used automatically by the software to determine the initial values.

Statistical analysis

To choose the best model, numerous statistical methods or error function analyses were utilized such as Ross's bias factor (BF) and accuracy factor (AF) [36], which is a non-penalty method for the number of the parameters of models and penalty-imposing methods to the number of parameters of models such as corrected adjusted coefficient of determination (R^2), AICc (Akaike Information Criterion) and Root-Mean-Square Error (RMSE) [37].

RESULTS AND DISCUSSION

The bacterial growth curves have a sigmoidal shape at different mercury concentrations, with lag times between 7 and 9 hours (**Fig. 1**). Overall growth was decreased as mercury content was increased, with 0.1 mg/L practically completely interrupting bacterial growth. Curve fitting of ln transformed bacterial growth at various mercury concentrations utilizing the modified Gompertz model (**Fig. 2**) indicates a high degree of model fit with values of coefficient of determination or R^2 >0.95 for each curve. The model also demonstrates that an increase in mercury levels resulted in slower growth development rates and a lengthier lag time at all concentrations was observed.

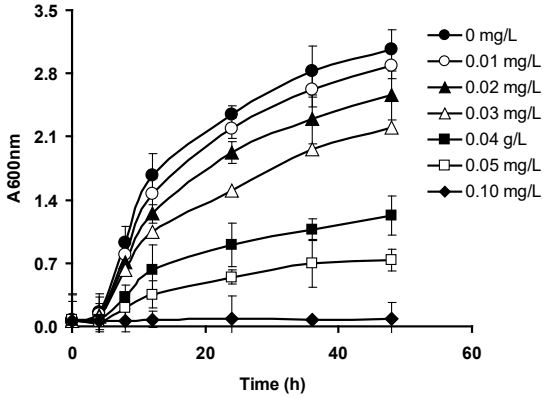

Fig. 1. Growth of *Pseudomonas* sp. strain DrY Kertih at 1.0 g/L acrylamide in the presence of mercury. The error bars are triplicate measurements of the mean ± standard deviation.

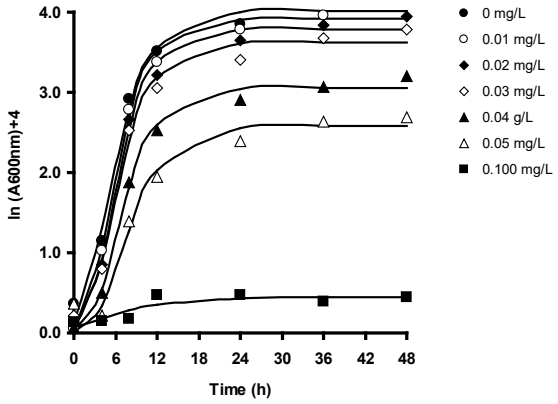

Fig. 2. Growth (natural log-transformed) of *Pseudomonas* sp. strain DrY Kertih at 1.0 g/L acrylamide in the presence of mercury as modelled using the modified Gompertz model.

The growth rates data at a range of mercury concentrations was then modelled using the Wang, Shukor, modified Han-Levenspiel, and modified Andrew, Kai and Liu models. The Amor model was unable to fit the data (**Figs. 3** to **8**).

Acceptable fitting is seen in the Wang, Shukor and modified Han-Levenspiel models, but poor fitting for the rest of the models. Statistical analysis showed that the Wang model was the best model. This is based on *RMSE* and AICc's lowest values, the highest adjusted correlation coefficient (adR^2) and the closest to unity for AF and BF (**Table 2**).

Table 2. Error function analysis for all models.

Model	*p*	RMSE	R^2	adR^2	AF	BF	AICc
Wang	3	0.01	0.99	0.99	1.02	1.00	-28.91
Modified Hans-Levenspiel	3	0.04	0.94	0.88	1.07	1.01	-13.96
Liu	2	0.09	0.27	-0.09	1.12	0.96	-17.62
Modified Andrews	3	0.06	0.86	0.72	2.46	0.41	-10.18
Shukor	3	0.04	0.96	0.92	1.06	1.01	-16.77
Kai	2	0.07	0.72	0.58	1.10	0.97	-21.91

Note:
adR^2 adjusted correlation coefficient
RMSE Root mean square error
AICc corrected Akaike Information Criteria
AF Accuracy factor
BF Bias factor
n.a. not available
p no of parameter

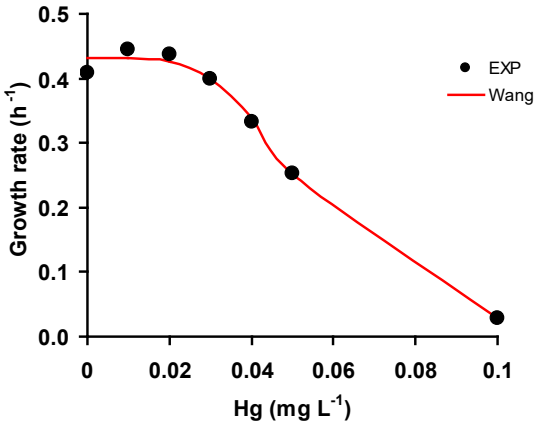

Fig. 3. Inhibitory effect of increasing concentrations of mercury to the bacterium's specific growth rate as modelled to Wang's model.

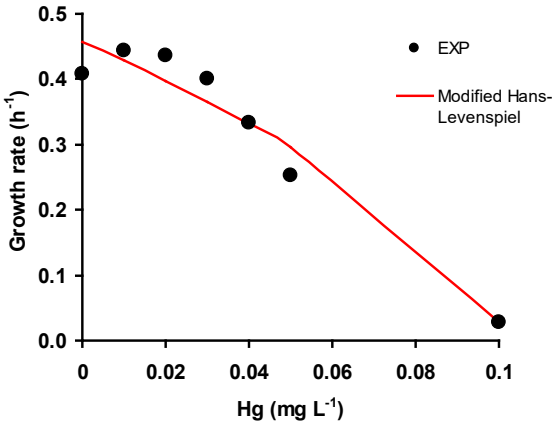

Fig. 4. Inhibitory effect of increasing concentrations of mercury on the bacterium's specific growth rate as modelled to the modified Hans-Levenspiel's model.

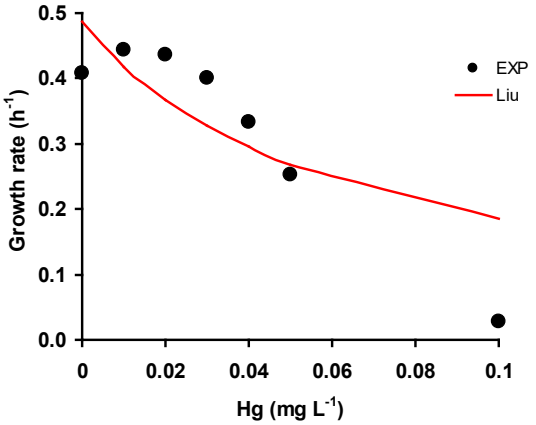

Fig. 5. Inhibitory effect of increasing concentrations of mercury on the bacterium's specific growth rate as modelled to Liu's model.

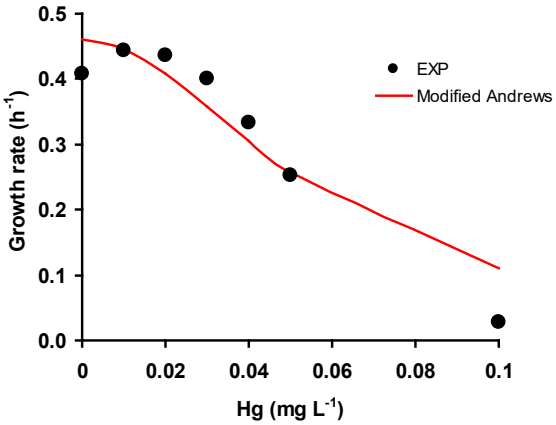

Fig. 6. Inhibitory effect of increasing concentrations of mercury to the bacterium's specific growth rate as modelled to the modified Andrew's model.

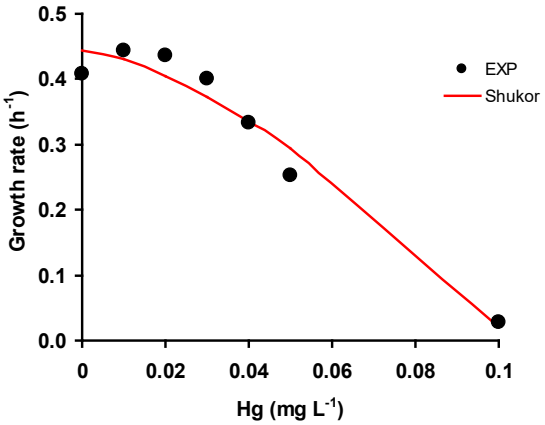

Fig. 7. Inhibitory effect of increasing concentrations of mercury on the bacterium's specific growth rate as modelled to the Shukor's model.

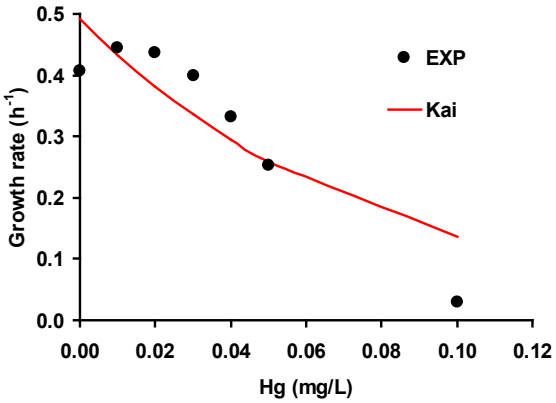

Fig. 8. Inhibitory effect of increasing concentrations of mercury on the bacterium's specific growth rate as modelled to the Kai model.

The parameters of the various models including the Wang model are shown in **Table 3**. Wang's model parameters were K_C, μ_{max} and m which represent inhibition constant (mg/L), maximum growth rate (per h) and empirical constant values were 0.054 mg/L, 0.431 h^{-1} and 4.295, respectively. Applying laboratory results in the field is greatly aided by Wang's model, which allows for the prediction of the heavy metals concentration that suppresses 50% of bacterial growth rate on toxicants.

Table 3. Parameter values for growth rate inhibition models.

Model	Value	95% Confidence Interval
Shukor		
μ_{max}	0.443	0.369 to 0.518
C_{crit},	0.103	0.087 to 0.120
n	1.494	0.571 to 2.416
Wang		
μ_{max}	0.431	0.407 to 0.455
K_C	0.054	0.049 to 0.059
m	4.295	2.691 to 5.899
Modified Han–Levenspiel		
μ_{max}	0.457	0.369 to 0.545
C_{crit},	0.101	0.091 to 0.112
m	0.637	0.002 to 1.272
Liu		
μ_{max}	0.486	0.287 to 0.685
K_C	0.062	-0.030 to 0.154
Amor	n.a.	n.a.
μ_{max}	n.a.	n.a.
K_i	n.a.	n.a.
Modified Andrews		
μ_{max}	127.303	-1116064 to 1116319
K_s	276.749	-2426316 to 2426870
K_i	Too large	
Kai		
μ_{max}	0.493	0.351 to 0.635
K	12.836	2.495 to 23.177

Despite the necessity of studying metal ions inhibition given that metal ions are found in polluted waterways with organic pollutants, such research is underrepresented in the literature. Only a small number of research have investigated how exposure to heavy metals affects the reproduction of bacteria in hazardous environments.

The inhibitory effects of metal ion on the growth or degradation rate of microorganisms is poorly modelled despite the importance of the outcome in identifying whether a certain inhibitor either partially or completely inhibited rates of growth or degradation. For instance, zinc and nickel ions strongly hindered the rate of the biodegradation of the xenobiotics monoaromatic hydrocarbons by two bacteria; *Bacillus* sp. and *Pseudomonas* sp.

The best model governing the inhibitory kinetics is the Andrews model which efficiently predicts the inhibitory influence of these ions on the rate of degradation [17]. To date, one of the most popular models utilized in modelling the effect of inhibitors be them metal ions, organic or inorganic on the growth of compounds, production of metabolites or degradation rate of pollutants is the modified Han-Levenspiel model where its application has been reported [16,38–42].

Heavy metals bind to critical functional groups impairing the enzyme activity. A critical functional group such as the sulfhydryl group is most easily bound [18]. When metal ions bind to the sulfhydryl (-SH) groups in active sites of enzymes necessary for microbial metabolic reactions, poisoning of the metabolic pathway results. In fact, the dissociation constant of a metal sulfide has been found to be inversely proportional to the minimum inhibitory concentration or MIC of that metal against *Escherichia coli* (Nies 1999). Metal ions may impede the degradation of pollutants or the production of industrially useful products such as hydrogen or methane by interfering with enzymes including dehydrogenases and oxygenases, which are broadly involved in metabolisms of xenobiotics. There are several strategies for allowing the biodegradation process to proceed in the occurrence of heavy metal ions that impede the process.

A metal-resistant bacterium's presence as a co-degrader can accelerate the breakdown process when paired with a main bacterial degrader. In one study, 2,4-D-soil polluted with cadmium was inoculated with the cadmium-resistant bacterium *Pseudomonas* H1, which efficiently sequestered cadmium in the cytoplasm, and a 2,4-D-degrading bacterium added to the targeted toxicant allows biodegradation process to proceed in soil microcosms studies. According to the study, inoculating a system with a cadmium-resistant bacterium allows the cadmium concentration in the soil to be not bioavailable for inhibiting xenobiotics-degrading bacterium in the neighbouring environment, promotes the biodegradation of the targeted organic contaminant [43].

Clay minerals are another option. These minerals are able to sorb heavy metal ions and have been used to decrease the bioavailability of metals and, thus, their toxicity. Clay minerals absorb heavy metals by a number of intricate adsorption methods, including surface complexation, direct bonding of metals to the surface of the clay mineral, and ion exchange. For instance, the toxicity of cadmium was mitigated for bacteria, yeasts, and an actinomycete when kaolinite (1-20%) or montmorillonite (1-5%) was added to an agar media containing cadmium [44]. Likewise, in one study, it is reported that cadmium toxicity to *Streptomyces bottropensis* is reduced by the addition of the clay minerals vermiculite and 3% bentonite [45]. To lessen the bioavailability and mobility of metals, additional soil treatment using chemicals such as phosphate, calcium carbonate, manganese oxide, cement, and magnesium hydroxide can be applied [46].

CONCLUSION

In conclusion, despite the necessity of studying the influence of metal ions, which is usually an inhibitor to the growth rate of bacteria biodegrading toxic substances, the use of metal inhibition models to represent such an effect is uncommon and widely overlooked. The Wang model was found to be the most successful of various metal inhibition models used for the effect of mercury on the growth of an acrylamide-degrading bacterium in this investigation. The Wang model provides for the estimation of the concentration of heavy metals necessary to halt 50% of bacterial growth rate on toxicants. Because the bacterium will have to deal with the toxicity of two types of toxicants at once, that is the metal and the targeted toxicant to be degraded, which is also toxic to the bacterium, it is predicted that the growth rate on toxic material will be even more significantly influenced. This research has significant implications for field trial efforts pursuing acrylamide bioremediation in mercury-contaminated areas.

REFERENCES

1. Spencer P, Schaumburg HH. Nervous system degeneration produced by acrylamide monomer. Environ Health Perspect. 1975 Jun 1;11:129–33.
2. Sega GA, Valdivia Alcota RP, Tancongco CP, Brimer PA. Acrylamide binding to the DNA and protamine of spermiogenic stages in the mouse and its relationship to genetic damage. Mutat Res Mutagen Relat Subj. 1989 Aug 1;216(4):221–30.
3. Tyl RW, Friedman MA. Effects of acrylamide on rodent reproductive performance. Reprod Toxicol. 2003 Jan 1;17(1):1–13.
4. Yang HJ, Lee SH, Jin Y, Choi JH, Han CH, Lee MH. Genotoxicity and toxicological effects of acrylamide on reproductive system in male rats. J Vet Sci. 2005 Jun;6(2):103–9.
5. Backer LC, Dearfield KL, Erexson GL, Campbell JA, Westbrook-Collins B, Allen JW. The effects of acrylamide on mouse germ-line and somatic cell chromosomes. Environ Mol Mutagen. 1989;13(3):218–26.
6. Hagmar L, Törnqvist M, Nordander C, Rosén I, Bruze M, Kautiainen A, et al. Health effects of occupational exposure to acrylamide using hemoglobin adducts as biomarkers of internal dose. Scand J Work Environ Health. 2001;27(4):219–26.
7. Igisu H, Goto I, Kawamura Y, Kato M, Izumi K. Acrylamide encephaloneuropathy due to well water pollution. J Neurol Neurosurg Psychiatry. 1975;38(6):581–4.
8. Mottram, DS, Wedzicha BL, Dobson AT. Acrylamide is formed in the Maillard reaction. Nature. 2002;419:448–9.
9. Shukor MY, Gusmanizar N, Azmi NA, Hamid M, Ramli J, Shamaan NA, et al. Isolation and characterization of an acrylamide-degrading *Bacillus cereus*. J Enviromental Biol. 2009;30(1):57–64.
10. Wang J, Wan W. Kinetic models for fermentative hydrogen production: a review. Int J Hydrog Energy. 2009;34(8):3313–23.
11. Manogaran M, Othman AR, Shukor MY, Halmi MIE. Modelling the Effect of Heavy Metal on the Growth Rate of an SDS-degrading *Pseudomonas* sp. strain DRY15 from Antarctic soil. Bioremediation Sci Technol Res. 2019 Jul 31;7(1):41–5.
12. Wang Y, Zhao QB, Mu Y, Yu HQ, Harada H, Li YY. Biohydrogen production with mixed anaerobic cultures in the presence of high-concentration acetate. Int J Hydrog Energy. 2008;33(4):1164–71.
13. Andrews JF. A mathematical model for the continuous culture of microorganisms utilizing inhibitory substrates. Biotechnol Bioeng. 1968 Nov 1;10(6):707–23.
14. Liu X, Zhu Y, Yang ST. Construction and characterization of ack deleted mutant of *Clostridium tyrobutyricum* for enhanced butyric acid and hydrogen production. Biotechnol Prog. 2006;22(5):1265–75.
15. Kai E, Lutfi W, Wan Johari WL, Habib S, Yasid N, Aqlima S, et al. The growth of the Rhodococcus sp. on diesel fuel under the effect of heavy metals and different concentrations of zinc. Adv Polar Sci. 2020 Jun 1;31:132–6.
16. Gąszczak A, Szczyrba E, Szczotka A, Greń I. Effect of Nickel as Stress Factor on Phenol Biodegradation by Stenotrophomonas maltophilia KB2. Materials. 2021 Jan;14(20):6058.

17. Amor L, Kennes C, Veiga MC. Kinetics of inhibition in the biodegradation of monoaromatic hydrocarbons in presence of heavy metals. Bioresour Technol. 2001 Jun 1;78(2):181–5.
18. Gopinath KP, Kathiravan MN, Srinivasan R, Sankaranarayanan S. Evaluation and elimination of inhibitory effects of salts and heavy metal ions on biodegradation of Congo red by *Pseudomonas* sp. mutant. Bioresour Technol. 2011;102(4):3687–93.
19. Abubakar A, Uba G, Biu HA. Kinetics Modelling of Pseudomonas stutzeri strain DN2 Growth Behaviour in Tributyltin Chloride. J Environ Microbiol Toxicol. 2021 Dec 31;9(2):13–8.
20. Abubakar A. Kinetics Modelling of Tributyltin Toxicity on The Growth of Bacillus subtilis. J Biochem Microbiol Biotechnol. 2021 Jul 30;9(1):19–24.
21. Abubakar A, Ibrahim S, Garba IK, Tanko AS, Abdulrasheed M, Adamu A, et al. Kinetics Modelling of Tributyltin Toxicity on The Growth of *Bacillus stearothermophilus*. Bioremediation Sci Technol Res. 2020 Jul 31;8(1):7–10.
22. Rahman MF, Rusnam M, Gusmanizar N, Masdor NA, Lee CH, Shukor MS, et al. Molybdate-reducing and SDS-degrading *Enterobacter* sp. strain Neni-13. Nova Biotechnol Chim. 2016;15(2):166–81.
23. Rusnam M, Gusmanizar N. Characterization of the growth on SDS by *Enterobacter* sp. strain Neni-13. J Biochem Microbiol Biotechnol. 2017 Dec 31;5(2):28–32.
24. Abubakar A, Gusmanizar N, Rusnam M, Syed MA, Shamaan NA, Shukor MY. Remodelling the Growth Inhibition Kinetics of Pseudomonas sp. Strain DrY Kertih on Acrylamide. Bioremediation Sci Technol Res. 2020 Dec 31;8(2):16–20.
25. Masdor N, Abd Shukor MS, Khan A, Bin Halmi MIE, Abdullah SRS, Shamaan NA, et al. Isolation and characterization of a molybdenum-reducing and SDS- degrading *Klebsiella oxytoca* strain Aft-7 and its bioremediation application in the environment. Biodiversitas. 2015;16(2):238–46.
26. Shukor MS, Shukor MY. A microplate format for characterizing the growth of molybdenum-reducing bacteria. J Environ Microbiol Toxicol. 2014;2(2):42–4.
27. Aisami A, Gusmanizar N. Characterization of an acrylamide-degrading bacterium isolated from hydrocarbon sludge. Bioremediation Sci Technol Res. 2019 Dec 28;7(2):15–9.
28. Wang Y, Fan Y, Gu JD. Dimethyl phthalate ester degradation by two planktonic and immobilized bacterial consortia. Int Biodeterior Biodegrad. 2004;53(2):93–101.
29. Wang GL, Li XF, Zhang H, Xiong MH, Li F. Optimization of CTN-4 to chlorothalonil-degrading conditions and a kinetics model. Zhongguo Huanjing KexueChina Environ Sci. 2013;33(11):1999–2005.
30. Mand TD, Döpfer D, Ingham B, Ané C, Kaspar CW. Growth and survival parameter estimates and relation to RpoS levels in serotype O157: H7 and non-O157 Shiga toxin-producing *Escherichia coli*. J Appl Microbiol. 2013;114(1):242–55.
31. Calvayrac C, Romdhane S, Barthelmebs L, Rocaboy E, Cooper JF, Bertrand C. Growth abilities and phenotype stability of a sulcotrione-degrading *Pseudomonas* sp. isolated from soil. Int Biodeterior Biodegrad. 2014;91:104–10.
32. Augustine A, Imelda J, Paulraj R, David NS. Growth kinetic profiles of *Aspergillus niger* S14 a mangrove isolate and *Aspergillus oryzae* NCIM 1212 in solid state fermentation. Indian J Fish. 2015;62(3):100–6.
33. Christen P, Vega A, Casalot L, Simon G, Auria R. Kinetics of aerobic phenol biodegradation by the acidophilic and hyperthermophilic archaeon *Sulfolobus solfataricus* 98/2. Biochem Eng J. 2012;62:56–61.
34. Basak B, Bhunia B, Dutta S, Chakraborty S, Dey A. Kinetics of phenol biodegradation at high concentration by a metabolically versatile isolated yeast *Candida tropicalis* PHB5. Environ Sci Pollut Res. 2014;21(2):1444–54.
35. Halmi MIE, Shukor MS, Johari WLW, Shukor MY. Mathematical modeling of the growth kinetics of *Bacillus* sp. on tannery effluent containing chromate. J Environ Bioremediation Toxicol. 2014;2(1):6–10.
36. Ross T. Indices for performance evaluation of predictive models in food microbiology. J Appl Bacteriol. 1996;81(5):501–8.
37. Halmi MIE, Shukor MS, Johari WLW, Shukor MY. Evaluation of several mathematical models for fitting the growth of the algae *Dunaliella tertiolecta*. Asian J Plant Biol. 2014;2(1):1–6.
38. Yin Y, Song W, Wang J. Inhibitory effect of acetic acid on dark-fermentative hydrogen production. Bioresour Technol. 2022 Nov 1;364:128074.
39. Mohanraj S, Anbalagan K, Rajaguru P, Pugalenthi V. Effects of phytogenic copper nanoparticles on fermentative hydrogen production by Enterobacter cloacae and Clostridium acetobutylicum. Int J Hydrog Energy. 2016 Jul 6;41(25):10639–45.
40. Gou C, Guo J, Lian J, Guo Y, Jiang Z, Yue L, et al. Characteristics and kinetics of biohydrogen production with Ni2+ using hydrogen-producing bacteria. Int J Hydrog Energy. 2015 Jan 5;40(1):161–7.
41. Wang J, Yin Y. Kinetic Models for Hydrogen Production. In: Wang J, Yin Y, editors. Biohydrogen Production from Organic Wastes [Internet]. Singapore: Springer; 2017 [cited 2023 Nov 7]. p. 269–90. (Green Energy and Technology). Available from: https://doi.org/10.1007/978-981-10-4675-9_6
42. Wang B, Wan W, Wang J. Inhibitory effect of ethanol, acetic acid, propionic acid and butyric acid on fermentative hydrogen production. Int J Hydrog Energy. 2008 Dec 1;33(23):7013–9.
43. Roane TM, Josephson KL, Pepper IL. Dual-Bioaugmentation Strategy To Enhance Remediation of Cocontaminated Soil. Appl Environ Microbiol. 2001 Jul;67(7):3208–15.
44. Babich H, Stotzky G. Effect of Cadmium on Fungi and on Interactions Between Fungi and Bacteria in Soil: Influence of Clay Minerals and pH. Appl Environ Microbiol. 1977 May;33(5):1059–66.
45. Kamel Z. Toxicity of cadmium to twoStreptomyces species as affected by clay minerals. Plant Soil. 1986 Jun 1;93(2):195–203.
46. Hettiarachchi GM, Pierzynski GM, Ransom MD. In situ stabilization of soil lead using phosphorus and manganese oxide. Environ Sci Technol. 2000;34(21):4614–9.